HHS Public Access

Author manuscript

Sci Immunol. Author manuscript; available in PMC 2018 February 02.

Published in final edited form as:

Sci Immunol. 2018 January 12; 3(19): . doi:10.1126/sciimmunol.aal2736.

Production of BMP4 by endothelial cells is crucial for endogenous thymic regeneration

Tobias Wertheimer[1,2,^], **Enrico Velardi**[1,^], **Jennifer Tsai**[1,3,^], **Kirsten Cooper**[3], **Shiyun Xiao**[4], **Christopher C. Kloss**[5,6,#], **Katja J. Ottmüller**[7], **Zeinab Mokhtari**[7], **Christian Brede**[7], **Paul deRoos**[3], **Sinéad Kinsella**[3], **Brisa Palikuqi**[5], **Michael Ginsberg**[8], **Lauren F. Young**[1], **Fabiana Kreines**[1], **Sophia R. Lieberman**[1], **Amina Lazrak**[1], **Peipei Guo**[5], **Florent Malard**[1], **Odette M. Smith**[1], **Yusuke Shono**[1], **Robert R. Jenq**[9], **Alan M. Hanash**[9], **Daniel J. Nolan**[8], **Jason M. Butler**[5], **Andreas Beilhack**[7], **Nancy R. Manley**[4], **Shahin Rafii**[5], **Jarrod A Dudakov**[3,10,†,*], and **Marcel RM van den Brink**[1,9,†,*]

[1]Immunology Program, Memorial Sloan Kettering Cancer Center, New York, NY 10065

[2]Division of Hematology and Oncology, Department of Medicine, Freiburg University Medical Center, Albert-Ludwigs-University, 79106 Freiburg, Germany

[3]Program in Immunology, Clinical Research Division, Fred Hutchinson Cancer Research Center, Seattle, WA 98109

[4]Department of Genetics, University of Georgia, Athens, GA 30602

[5]Department of Genetic Medicine and Ansary Stem Cell Institute, Weill Cornell Medical College, New York, NY 10021

[6]Center for Cell Engineering, Memorial Sloan Kettering Cancer Center, New York, NY 10065

[7]Department of Medicine II, Wurzburg University Hospital, Interdisciplinary Center for Clinical Research (IZKF), and Graduate School of Life Sciences, Wurzburg, Germany

[8]Angiocrine Biosciences, San Diego, CA 92130

[9]Department of Medicine, Memorial Sloan Kettering Cancer Center, New York, NY 10065

[10]Department of Immunology, University of Washington, Seattle, WA 98109

Abstract

[*]Address correspondence to jdudakov@fredhutch.org or vandenbm@mskcc.org.

[^]T.W., E.V., and J.T. contributed equally

[†]J.A.D and M.R.M.vdB contributed equally toward directing the work

[#]Current address: Center for Cellular Immunotherapies and Parker Institute for Cancer Immunotherapy, Perelman School of Medicine, University of Pennsylvania, PA 19104.

Author contributions: T.W., E.V., and J.T. contributed to the design, execution, analysis and interpretation of the studies and drafting of the manuscript; S.X. performed studies on iGrem^{TEC} mice under the guidance of N.R.M.; K.C. performed bioinformatics and *in vitro* studies; C.C.K. assisted in the identification of thymic ECs; B.P., K.O., Z.M. and C.B. performed imaging studies on thymic vasculature under the guidance of A.B. and S.R; M.G., P.G., and C.C.K. provided exECs and guidance on their generation supervised by D.N., J.B., and S.R; L.F.Y., F.K, S.R.L., A.L., O.M.S., Y.S., R.R.J., and A.M.H performed, analyzed and helped interpret experiments. J.A.D. and M.R.M.vdB designed, interpreted and supervised all studies and wrote the manuscript. All authors contributed towards editing the manuscript.

Data and materials availability: The microarray data used in this study have been deposited in the GEO under accession number GSE106982.

The thymus is extremely sensitive to damage but also has a remarkable ability to repair itself. However, the mechanisms underlying this endogenous regeneration remain poorly understood and this capacity diminishes considerably with age. Here we show that thymic endothelial cells (ECs) comprise a critical pathway of regeneration, via their production of BMP4. ECs increased their production of BMP4 after thymic damage, and abrogating BMP4 signalling or production by either pharmacologic or genetic inhibition impaired thymic repair. EC-derived BMP4 acted on thymic epithelial cells (TECs) to increase their expression of *Foxn1*, a key transcription factor involved in TEC development, maintenance and regeneration; and its downstream targets such as *Dll4*, itself a key mediator of thymocyte development and regeneration. These studies demonstrate the importance of the BMP4 pathway in endogenous tissue regeneration and offer a potential clinical approach to enhance T cell immunity.

Continuous generation of adaptive immune diversity is dependent on T cell development in the thymus. T cell development is a complex process involving the continuous differentiation and development of thymocytes in close interaction with, and under the instruction of, the surrounding stromal microenvironment; which is comprised of endothelial cells (ECs), fibroblasts, and highly specialized thymic epithelial cells (TECs). Signals stemming from the microenvironment that drive T cell development include the Notch ligand Delta-like 4 (DLL4); cytokines such as interleukin-7 (IL-7) and stem cell factor (SCF); as well as chemokines such as CXCL12, CCL19, CCL21, and CCL25 (1).

Notwithstanding its importance for generating and maintaining an important arm of adaptive immunity, the thymus is extremely sensitive to damage, which can come in the form of stress (corticosteroids), cytoreductive chemotherapy, infection, sex hormones, surgery, and irradiation (2); but it also has a remarkable capacity for repair. In fact, the general phenomenon of endogenous thymic regeneration has been known for longer even than its immunological function (3, 4), however, the underlying mechanisms controlling this process remain unstudied. Although there is likely continual thymic involution and regeneration in response to stress and infection in otherwise healthy people, acute and profound thymic damage such as that caused by common cancer cytoreductive therapies or the conditioning regimes as part of hematopoietic cell transplantation (HCT), leads to prolonged T cell deficiency; precipitating high morbidity and mortality from opportunistic infections and may even facilitate cancer relapse (5, 6). Furthermore, the continuous decline in thymic function with age drastically erodes the regenerative capacity of the thymus (2, 7). There is therefore a clear clinical need for therapeutic strategies to mediate rapid regeneration of thymic function following acute immune damage.

One approach to developing novel regenerative strategies is to understand and exploit the pathways underlying endogenous thymic regeneration. We have recently described one such pathway centered on the production of interleukin-22 (IL-22) by innate lymphoid cells (ILCs) (8). IL-22 is significantly upregulated after damage and mice deficient for IL-22 had a defect in their thymic regenerative capacity (8). However, while *Il22*$^{-/-}$ animals lagged behind wildtype controls in their ability to repair thymus function, there was still considerable regeneration in IL-22-deficient mice (8), suggesting that other pathways likely play a role during endogenous thymic regeneration.

RESULTS

BMP signaling pathways are upregulated after thymic damage

To identify alternate regeneration pathways in the thymus, we performed an unbiased transcriptome analysis of the non-hematopoietic ($CD45^-$) stromal cell compartment of the thymus, which is less sensitive to thymic damage compared to the $CD45^+$ hematopoietic compartment (Supplementary Fig. 1A). In order to detect gene changes likely important for regeneration, we focused on days 4 and day 7 after a sublethal dose of total body irradiation (TBI); critical timepoints that immediately precede observable cellular regeneration (day 4), and when significant but incomplete regeneration is underway (day 7) (Supplementary Fig. 1B). Using this approach we found significant upregulation at both days 4 and 7 of several genes known to be involved in thymic function, including *Foxn1*, *Dll4, Kitl, Cxcl12, Il7*, and *Fgf7* (Fig. 1A); many of which have been described to promote thymic regeneration when given exogenously or activated genetically (2). However, in addition to these canonical thymopoietic factors, we also found significant upregulation of *Bmp4*, which is a critical factor during the development of multiple organs, including the thymus where it can target both stromal and hematopoietic compartments (9). Reflecting this increase in *Bmp4* expression, we could also identify a significant enrichment at both day 4 and 7 after TBI in genes downstream of BMPR signaling (GO: 0030510) (Fig. 1B). These gene changes were confirmed at the protein level by a significant increase in the intrathymic levels of BMP4 from day 7 to day 14 after TBI (Fig. 1C). However, although the absolute levels of BMP4 do not increase until day 7, reflecting the increase in BMP signaling observed prior to the increase in absolute BMP4 (Fig. 1B–C), we found a significant increase in the relative amounts of BMP4, suggesting an increase in the bioavailability of BMP4 as early as day 2 (Fig. 1D). Consistent with a localized effect, mice that received targeted irradiation to the mediastinum (which locally targets the region encompassing the thymus) also have increased availability of BMP4 (Supplementary Fig. 1C). Together, these findings suggest that BMP signaling pathways are activated during the regenerative response in the thymus after damage.

BMP4 induces TECs to upregulate Foxn1 and its downstream targets after damage

The cognate receptor for BMP4 is a heterodimer made up of two subunits: a non-redundant Type II receptor, BMPR2, and one of two type I receptors BMPR1A or BMPR1B, which signal through Smad1/5/8 (10). Analysis of the cellular distribution of these receptor subunits revealed widespread expression in the thymus, although non-hematopoietic stromal cells expressed *Bmpr1a* 2–3 logs higher than thymocytes (Supplementary Fig. 2). Interestingly, although there was detectable expression of *Bmpr1a* and *Bmpr2* by all TEC subsets, higher expression of the non-redundant *Bmpr2* subunit was detected on cTECs compared to mTECs (Fig. 2A). BMP4 signals can also contribute to the differentiation of pluripotent stem cells towards the TEC lineage (11, 12), possibly via its ability to directly induce upregulation of FOXN1 (13), a forkhead box transcription factor that is not only critical for TEC development and maintenance (14, 15), but can even confer TEC identity on cells such as fibroblasts (16). Consistent with the differential expression of the *Bmpr2* by TECs, we found that *Foxn1* expression was significantly increased at day 4 and 7 after TBI in purified cTECs, but not mTECs (Fig. 2B). Although the non-redundant function for

FOXN1 in the thymus has been known for decades (14, 17), its role in regeneration is only beginning to be understood (18, 19). Consistent with a role for FOXN1 during endogenous thymic regeneration, we found significant changes at days 4 and 7 after TBI in expression of a large proportion of the FOXN1 targets identified by the Boehm and Hollander groups (20–22). Specifically, 66% and 68% of FOXN1 targets were significantly changed at days 4 and 7, respectively, and 79% were significantly changed at either day 4 or day 7 after TBI (Table S1; Fig. 2C–D). Subsequent GSEA analysis confirmed these findings showing a significant enrichment in these downstream FOXN1 targets at both day 4 and 7 after thymic damage (Fig. 2E). Although there was a significant increase in *Foxn1* expression between day 4 and 7 in cTECs (Fig. 2B), we did not observe a considerable change in FOXN1 target gene expression between days 4 and 7 after TBI (Fig. 2C–E).

BMP4 produced by ECs is a critical mediator of endogenous thymic regeneration

Consistent with our hypothesis that BMP signaling is important during endogenous thymic regeneration, mice treated with the pan BMP inhibitor Dorsomorphin dihydrochloride (12.5mg/kg) beginning 1 day prior to TBI exhibited significantly worse thymic recovery compared to PBS treated controls (Fig. 3A), including all thymocyte and stromal populations analyzed (Supplementary Fig. 3A–B). To confirm these pharmacologic findings, we generated iGremlin::K5-CreER^{+} (iGrem^{TEC}) mice, in which expression of the secreted BMP inhibitor Gremlin is induced by CreER driven by the Keratin 5 promoter leading to tamoxifen-induced expression of Gremlin in mTECs. Upon tamoxifen administration these mice exhibited significantly worse thymic regeneration after TBI compared to iGremlin::K5-CreER^{-} (iGrem^{WT}) control mice (Fig. 3B, Supplementary Fig. 3C–D).

To determine the cellular source of BMP4 in the thymus, we FACS purified cell populations comprising 99.5% of the thymus (including all thymocyte subsets, TECs, dendritic cells (DCs), ECs and fibroblasts) at steady state and measured expression of *Bmp4* by qPCR. This analysis revealed that the only cell subsets within the thymus to produce detectable levels of *Bmp4* mRNA were fibroblasts and ECs (Fig. 3C). However, when we FACS purified these two populations at days 0 and 4, ECs but not fibroblasts exhibited an increased expression of *Bmp4* (Fig. 3D). Pharmacologic inhibition of BMP signaling using dorsomorphin dihydrochloride inhibits multiple BMP signaling pathways while induction of Gremlin inhibits signaling from BMP-2, -4, and -7. To conclusively determine the role of EC-derived BMP4 during thymic regeneration, BMP4$^{fl/fl}$ mice were crossed with Cdh5(PAC)-CreERT2 mice (BMP4$^{\Delta EC}$), enabling tamoxifen-induced deletion of BMP4 specifically in ECs (Supplementary Fig. 4A–B), which express Cdh5 (VE-Cadherin) (23). Although there was no immediate loss in thymic function when BMP4 was deleted at baseline (Supplementary Fig. 4C), if BMP4 was deleted immediately prior to TBI there was a significant loss of thymic recovery compared to controls (Fig. 3E, Supplementary Fig. 4D).

ECs represent a damage-resistant niche within the thymus

Our previous data revealed that ILCs, which can contribute towards endogenous thymic regeneration, were extremely damage-resistant (8). We analyzed the depletion of most cell subsets within the thymus 7 days after exposure to TBI, and found that along with ILCs, ECs were resistant to acute thymic injury (Fig. 4A). This finding is consistent with previous

studies demonstrating that thymic ECs are resistant to damage (24). To confirm this finding, we analysed ECs after damage caused by cytoreductive chemotherapy, corticosteroids or TBI, at a timepoint that is at the nadir of cellularity (Supplementary Fig. 5A) and results in extensive depletion of all subsets of thymocytes and TECs (Supplementary Fig. 5B–D). In each of these models we found that the number of ECs in the thymus remained remarkably unchanged (Fig. 4B), resulting in an increase in the proportion of these cells as the cellularity of the thymus decreased (Fig. 4C). Using TBI as a model of thymic damage (Supplementary Fig. 1B), we found that there was no change over time in the absolute number of ECs measured by flow cytometry (Fig. 4D). Furthermore, given the depletion of cells in the thymus, the proportion of ECs increased as a proportion of $CD45^-$ non-hematopoietic stromal cells (Fig. 4E) and total thymus cellularity (Fig. 4F). However, although there was no change in the absolute number of ECs, visualization using light-sheet fluorescence microscopy (LSFM) on the whole thymus after TBI revealed that the volume of the vasculature decreased commensurate to the rest of the thymus after damage (Fig. 4G–H; Supplementary movies). Reflecting this change in vascular volume, there was a significant decrease in the total number of vessel segments at days 4 and 7 after TBI, but this had largely returned to baseline levels by day 14 (Fig. 4I). Similarly, the length of each vessel segment was reduced significantly after TBI leading to a profound loss in total vessel length) but had begun regenerating by day 14 after TBI (Fig. 4J). Similarly, vessel branching, which is a critical vascular function, declines precipitously immediately after damage, slowly regenerating by day 14 (Fig. 4K–L). However, although there are profound changes to vascular architecture after damage, there was a significant increase in the density of the vasculature after TBI (Fig. 4M).

Administration of ex vivo propagated ECs promotes thymic regeneration in a BMP4-dependent fashion

Although the role of ECs during tissue regeneration has traditionally been attributed to their role in vascularization, including in the thymus (25), recent work has suggested that ECs can also contribute towards regeneration via their production of so-called angiocrine factors (26–28). Using a technique to constitutively activate the Akt pathway in ECs using the prosurvival adenoviral gene *E4ORF1* (29), ECs can be propagated and expanded *ex vivo* (exEC) while maintaining their phenotype and vascular tube formation capacity (Supplementary Fig. 6A–B). Consistent with this, GSEA analysis comparing transcriptomes derived from freshly isolated thymic ECs or $exEC^{(Thymus)}$ revealed no significant enrichment for gene signatures related to EC differentiation, branching, angiogenesis, or EC apoptosis (Supplementary Fig. 6C); although perhaps unsurprising given its constitutive activation of Akt (30), there was enrichment for genes associated with EC proliferation and mild enrichment for EC migration (Supplementary Fig. 6C). Intravenous (iv) administration of 1×10^6 exEC derived from the thymus ($exEC^{(Thymus)}$) 72 hours after TBI (Fig. 5A) led to significantly increased thymic cellularity compared to control mice on day 9 after irradiation (Fig. 5B). Although unchanged in their proportion (Fig. 5C–D), this increased cellularity was reflected within both TEC and thymocyte subsets (Fig. 5E, Supplementary Fig. 6D), driven, at least in part, by increased cTEC proliferation (Fig. 5F). These *in vivo* data support our *in vitro* studies, which showed that BMP4 could directly promote proliferation of C9 but not TE-71 TEC cell lines (representing cTECs and mTECs, respectively) (Fig. 5G). Taken

together, these data are consistent with the differential BMP4 receptor expression we had observed in TECs (Fig. 2A). Intriguingly, although considerable benefit to thymic regeneration was observed with exEC$^{(Thymus)}$, we observed no effect on thymus regeneration when exEC were derived from cardiac or kidney endothelial cells (exEC$^{(Heart)}$ or exEC$^{(Kidney)}$) (Fig. 5A–E), consistent with the previously demonstrated heterogeneity between ECs from different tissues and the tissue-specificity of EC-derived regeneration (31).

Using this model of exogenous administration, the total number of ECs in the thymus was also significantly increased in mice that received exEC$^{(Thymus)}$ (Fig. 5H). Interestingly, unlike TECs, we did not observe any change in EC proliferation after exEC$^{(Thymus)}$ administration (Fig. 5I). Taken together, this suggests that exEC derived from the thymus are preferentially able to enter the thymus to mediate regeneration. However to conclusively track the ability of exECs to enter the thymus, we transplanted 10×10^6 CFSE$^+$ exEC 72h after TBI. Using this approach, we could detect a small population of CFSE$^+$ ECs in the thymus at 4 hours after transfer (Fig. 5J). Supporting the notion that exEC$^{(Thymus)}$ do in fact get in to the thymus, we observed the same capacity for thymic regeneration when 100 times fewer cells were injected directly into the thymus compared to iv (Supplementary Fig. 6E). Moreover, this regenerative benefit of exEC administration was persistent as we could still detect increased cellularity within the thymus for at least 28 days after TBI (Fig. 5K).

Administration of exEC$^{(Thymus)}$ induced upregulation of *Foxn1* by TECs (Fig. 6A), but reflecting the differential expression of *Bmpr2* (Fig. 2A), this increase was only observed in cTECs and not mTECs. Indeed, highlighting this mechanism of regeneration, we also found significant upregulation of the FOXN1 target genes *Dll4*, *Kitl*, and *Cxcl12* (Fig. 6B), all of which are critical for steady state T cell development and reconstitution (20, 32–34). Even though our studies suggest that the effects of BMP4 are primarily restricted to cTECs, surprisingly, conditioned media (CM) from exEC$^{(Thymus)}$ induced Smad1/8 phosphorylation in both the C9 and TE-71 cell lines (Fig. 6C–D), indicating that either BMP4 can signal through mTECs but that its effects are independent of *Foxn1* and proliferation, or that additional factors in the CM could be inducing Smad1/8 phosphorylation.

Although expression of *Foxn1* decreases considerably when TECs are immortalized, including the C9 cTEC cell line (Supplementary Fig. 7A), its expression can be induced in C9 cells by BMP4 (Supplementary Fig. 7B). Supporting the hypothesis that BMP4 production by exECs leads to thymic regeneration via induction of FOXN1, incubation of C9 cells for 24 hours with CM from exEC$^{(Thymus)}$ was enough to induce expression of *Foxn1* in a similar fashion to recombinant BMP4 (Fig. 6E); an effect that could be abrogated with addition of the BMP inhibitor Noggin (Fig. 6E). Similar to our *in vivo* results, we found that CM from exEC$^{(Thymus)}$ led to upregulation of both *Dll4* and *Kitl* in C9 cells (Fig. 6F). Interestingly, exEC derived from the thymus expressed significantly more BMP4 (transcript and protein) compared to exEC derived from heart or kidney (Fig. 6G–H); and were subsequently able to induce *Foxn1* in C9 cells while exEC from kidney or heart were unable to induce *Foxn1* (Fig. 6I). Together these data offer an explanation for the differential thymic regenerative capacities of these populations.

Finally, to test the impact of BMP4 on exEC-mediated thymic regeneration, we generated exEC$^{(Thymus)}$ with BMP4 silenced by shRNA. As confirmed by qPCR, *Bmp4* expression was reduced approximately 90% in thymic exEC transduced with the shRNA, compared to the scrambled control (Supplementary Fig. 7C). Unlike CM from shScram, which induced *Foxn1* expression when incubated with C9 cells, CM from cultures of shBmp4 exEC failed to upregulate *Foxn1* (Fig. 6J) or its downstream targets *Dll4* and *Kitl* (Fig. 6K). In mice given TBI and treated with scrambled or shRNA exEC$^{(Thymus)}$ on day 3, we found that the increase observed when exEC$^{(Thymus)}$ were administered was abrogated if BMP4 was silenced in these cells (Fig. 6L).

DISCUSSION

Endogenous thymic regeneration is a critical process that allows for the renewal of immune competence after such everyday insults as stress and acute infection. However, prolonged thymic deficiency caused by age-related involution, repeated rounds of cytoreductive chemotherapy or chronic infection, is a significant clinical challenge that can lead to increased opportunistic infections, reduced response to vaccines, and decreased capacity for immune surveillance (2). Although there is a well-described role for BMP4 during thymus organogenesis (9, 35, 36), and BMP4 is a crucial mediator in the induction TEC-like cells from pluripotent stem cells (11, 12, 37), its postnatal role has not been well defined. Our findings demonstrate that ECs are a necessary postnatal source of BMP4 that drives thymic regeneration after injury, primarily via upregulation of the key TEC transcription factor FOXN1 and its downstream targets. Our findings support previous *in vitro* data linking BMP4 signaling and expression of *Foxn1* (13, 38).

FOXN1 is a forkhead box transcription factor expressed early during thymic ontogeny that is crucial for functionally enabling TECs to support T cell development (14, 39, 40). However, the role of FOXN1 is not restricted to the formation of thymus but is also critical for ongoing TEC maintenance and its declining expression likely contributes age-related thymic involution (15, 41–44). Furthermore, there is increasing evidence that FOXN1 is also important during thymic regeneration, as forced induction of FOXN1 is capable of reversing age-related thymic atrophy (18, 19) and recombinant FOXN1 protein can enhance T cell reconstitution after HCT (45). However, despite its importance for thymic function, it was only recently in a series of elegant studies by Hollander and colleagues that a comprehensive list of 450 high-confidence direct targets of FOXN1 were identified in cTECs (21). Importantly, this list of targets verified the four putative FOXN1 targets (*Dll4, Kitl, Ccl25*, and *Cxcl12*) that had been previously identified (20, 42). Consistent with the hypothesis that FOXN1 is a crucial regulator of endogenous regeneration, our studies demonstrated that *Foxn1* expression was increased in cTECs after damage, but also that there was a significant enrichment in expression of these direct FOXN1 target genes. Regulation of the Notch ligand DLL4 is particularly relevant for regeneration as, not only is it critically important for steady state thymic function with DLL4 deletion leading to complete abrogation of T cell development (33, 34), but we have previously shown that the concentration of intrathymic DLL4 expression can profoundly impact T cell development and thymus size (46).

Several recent studies have found that ECs, rather than merely passive conduits, can have an active role in tissue repair via production of so called angiocrine factors (28). Evidence for this regenerative role of ECs has been found in the liver (mediated by CXCR7, HGF and Wnt2) (27, 47), lung (mediated by MMP14) (26), and bone marrow hematopoiesis (mediated by Notch signaling) (48–50). In addition to providing further evidence of the endogenous tissue regeneration capacity of ECs, our studies in the thymus also propose a potential therapeutic strategy for promoting exogenous thymic regeneration using *ex vivo* propagated Akt-activated exECs (30). Reflecting the findings in lung and bone marrow (26, 48, 51), exEC administration could significantly promote thymic regeneration after acute injury; but only when the transferred exECs were derived from thymus and not other tissues such as the heart or kidney. These findings further highlight the high degree of EC tissue-specificity, particularly in their response to damage and role during regeneration (31). Further to the lymphostromal interactions that regulate T cell development and TEC function (1), there is a commensurate influence of TECs on EC function such that TEC-specific deletion of VEGF-A, or insertion of a hypomorphic FOXN1 allele, leads to disruption of the thymic vasculature (52, 53). Thus, while it is clear that ECs can promote TEC function and regeneration after damage, it will be interesting to study the role that TECs play in guiding EC function, including their tissue-specificity.

In both endogenous and exogenous regeneration models, our studies suggest that the effects of BMP4 are restricted mostly to cTECs, but not mTECs. Specifically, we found: 1) that in the endogenous setting of regeneration after TBI there is an increase in *Foxn1* expression in purified cTECs but not mTECs; 2) recombinant BMP4 induces expression of *Foxn1* and proliferation in the C9 (cTEC) but not the TE-71 (mTEC) cell line; and 3) exEC administration induces expression of *Foxn1* and leads to the proliferation of cTECs but not mTECs. These findings can be explained by enriched expression of the non-redundant *Bmpr2* receptor subunit on cTECs compared to mTECs. Given the identification of bipotent TEC progenitors (TEPC) during development and in the postnatal thymus that share common phenotypic cTEC markers (54–58), together with the capacity of BMP4 to drive TEC differentiation from pluripotent progenitors and stimulate postnatal TEPC (11, 12, 37, 59); it is possible that BMP4 stimulation of TEPC drives thymic regeneration. While there is evidence that at least one of these progenitor cells is not capable of robust postnatal maintenance and regenerative capacity (60), the relative contribution of these phenotypically distinct TEPC towards endogenous thymic regeneration is currently unclear and will require further study. Furthermore, at least one mechanism by which BMP4 can aid in thymic repair (namely, increased expression of *Foxn1* and its downstream targets such as *Dll4*) does not necessarily depend on direct stimulation of TEPC. However, even though our data strongly suggests that BMP4 signaling promotes thymic regeneration primarily by stimulating cTEC function, given that 1) BMP4 can regulate hematopoietic stem cell (HSC) function (61); 2) Akt-activated ECs can promote HSC function *in vitro* and *in vivo* (48, 50, 62); and 3) the input of hematopoietic progenitors from the BM is critical to maintain thymic function, and a limited supply of hematopoietic progenitors hinders T cell reconstitution after HCT (63); we cannot exclude the possibility that exECs have both direct and indirect effects in aiding thymic regeneration. Moreover, since we can only detect exEC transiently after transfer, it is not entirely clear if they mediate their effect locally or extrathymically. Nevertheless, the

requirement for exEC regeneration on BMP4 and our observance of similar downstream targets to those observed during BMP4-mediated endogenous regeneration, strongly suggests an equivalent mechanism of regeneration. More importantly, regardless of their local or systemic mechanisms, exEC and/or BMP4 represents a potent therapeutic strategy to improve thymic regeneration.

Furthermore, while BMP4 appears to be critical for promoting TEC regeneration after injury, given that BMP4 receptors are also expressed on some thymocyte populations, and BMP4 has been reported to inhibit the differentiation of T cells (64–67), the observation that BMP4 expression by ECs peaks early after damage and returns to baseline levels in both absolute and relative amounts by day 21, is likely significant for coordinating this balance of functions. Taken together, these studies not only identify a mechanism governing endogenous thymic regeneration, but also offer potential therapeutic strategies for immune regeneration in patients whose thymus has been irrevocably damaged. These strategies are novel candidates for therapies to enhance thymic regeneration and improving immune competence in patients whose thymic function has been compromised due to cytoreductive conditioning, infection or age.

METHODS

Study design

The goal of this study was to identify and understand mechanisms of endogenous thymic regeneration. The Institutional Animal Care and Use Committees at Memorial Sloan Kettering Cancer Center, the Fred Hutchinson Cancer Research Center, and the University of Georgia approved these studies. Power calculations from past studies were used to calculate the number of mice needed to ensure statistical power. All animal studies were conducted on three to twenty-five biological replicates. No randomization or blinding was performed but all results were confirmed by two or more independent experiments.

Mice

Inbred female C57BL/6 mice were obtained from the Jackson Laboratories (Bar Harbor, USA). BMP4$^{\Delta EC}$ mice were generated by crossing B6;129S4-*Bmp4*^{tm1Jfm}/J mice (obtained from Jackson Laboratories) with Cdh5(PAC)-CreERT2 (which were kindly provided by Dr Ralf Adams from the Max Planck Institute under an MTA through Cancer Research UK) (23). To induce deletion, Tamoxifen (Sigma) was dissolved in corn oil and administered intraperitoneally (ip) at a dose of 40mg/kg/day daily for 5 days starting 2 days before TBI. iGrem^{TEC} mice were generated by Nancy Manley (University of Georgia) by crossing K5-CreER mice with B6;129S1-Gt(ROSA)26Sor$^{tm1(Grem1)Svok}$ mice (which were kindly provided by Dr Steve Vokes at the University of Texas, Austin) (68). To induce expression of Gremlin, Tamoxifen was dissolved in corn oil and administered ip at a dose of 40mg/kg/day daily for 3 days starting 1 day before TBI.

To induce thymic damage, mice were given either sublethal TBI, cyclophosphamide (Cyclo) or dexamethasone (Dex). TBI was given at a dose of 550 cGy from a cesium source mouse irradiator with no hematopoietic rescue; Cyclo was administered ip in 2 doses of 100mg/kg

over 2 days; Dex was administered ip at a dose of 50mg/kg. The BMP type I receptor inhibitor dorsomorphin dihydrochloride was given to indicated mice at a dose of 12.5mg/kg one day before TBI and then twice daily from day 1. Mice were maintained at the Memorial Sloan Kettering Cancer Center (New York, USA), Fred Hutchinson Cancer Research Center (Seattle, WA) or at the University of Georgia (Athens, GA). Animals were allowed to acclimatize for at least 2 days before experimentation, which was performed according to Institutional Animal Care and Use Committee guidelines.

Reagents

For detection of BMP4, whole thymus lysates were prepared by homogenizing tissue in RIPA buffer (50 mM Tris pH 7.6, 150 mM NaCl, 1% NP-40, 1% SDS, 0.01% sodium deoxycholate, 0.5 mM EDTA, and protease inhibitors (Thermo, A32955). The resulting supernatant was quantified using the BMP4 ELISA kit (LSBio, LS-F13543) and read on a Spark 10M plate reader (Tecan, Switzerland). For flow cytometry and cell sorting, surface antibodies against CD45 (30-F11), CD31 (390 or MEC13.3), VE-Cadherin (BV13), TER-119 (TER-119), CD4 (RM4-5 or GK1.5), CD8 (53-6.7), TCRβ (H57-597), CD3 (145-2C11), ckit (2B8), CD25 (PC61), CD44 (IM7), IA/IE (M5/114.15.2), EpCAM (G8.8), Ly51 (6C3), CD11c (HL3), L-7Rα (A7R34), NKp46 (29A1.4), RORγt (B2D), CCR6 (140706), and PDGFRα (APA5) were purchased from BD Biosciences, BioLegend or eBioscience. Ulex europaeus agglutinin 1 (UEA-1), conjugated to FITC or Biotin, was purchased from Vector Laboratories (Burlingame, CA). Flow cytometric analysis was performed on an LSRII (BD Biosciences) and cells were sorted on an Aria II (BD Biosciences) using FACSDiva (BD Biosciences) or FlowJo (Treestar Software).

Cell Isolation

Individual or pooled single cell suspensions of freshly dissected thymuses were obtained and either mechanically suspended or enzymatically digested as previously described (8, 46). $CD45^-$ cells were enriched by magnetic bead separation using an AutoMACS (Miltenyi Biotech). To isolate or analyze thymic ECs, mice were anaesthetized with isoflurane, administered iv with BV13 antibody (anti-VE-Cadherin, 250μg/ml), and euthanized 15 minutes after injection.

Generation of exEC

exEC were generated as previously described (29). Briefly, $CD45^-$VE-$Cadherin^+$ cells were FACS purified and incubated with lentivirus containing the E4ORF1 construct for 48 hours. Cell culture medium containing murine recombinant VEGF (10ng/ml) and FGF-2 (20ng/ml), endothelial growth supplement (bovine hypothalamus) (Alfa Aesar), sb431542 (Tocris Biosciences), heparin (50μg/ml) (Sigma-Aldrich), 1% Glutamax (Life Technologies), 1% non-essential amino acids (Life Technologies), 1% HEPES Buffer (Life Technologies), 1% antibiotic-antimycotic (Life Technologies) was replaced every 48h.

Co-culture experiments

Culture medium that had been conditioned with exEC for 48h was incubated with C9 cells (kindly provided by A. Farr, University of Washington) for 40h. Recombinant murine BMP4

(30ng/ml) and recombinant murine Noggin (100ng/ml) were purchased from Peprotech (Rocky Hill, NJ). *In vitro* cell proliferation was measured using the CellTiter Non-Radioactive Cell Proliferation Assay (Promega)

Microarray

Thymic non-hematopoietic stromal cells were isolated using CD45 MACS cell depletion. Microarray analysis was performed on an Affymetrix MOE 430 A 2.0 platform in triplicate for untreated mice as well as day 4 and 7 after TBI. To obtain sufficient RNA for every timepoint, thymic ECs of several mice were pooled. All samples underwent a quality control on a bioanalyzer to exclude degradation of RNA. RNA extraction, control of RNA integrity with a bioanalyzer, and cRNA labeling and hybridization, was performed by the Integrated Genomics Core Facility of Memorial Sloan Kettering Cancer Center. GSEA analysis was performed using the GSEA tool v2.0 of the Broad Institute (http://software.broadinstitute.org/gsea). Comparisons were made to known signaling pathways from the Gene Ontogeny database (GO numbers: 0045446, 0010594, 0001938, 0001763, 0002040, 2000351, 0030510) as well as the list of published downstream FOXN1 targets (21). The microarray data used in this study have been deposited in the GEO under accession number GSE106982.

PCR

Reverse transcription-PCR was performed with QuantiTect reverse transcription kit (QIAGEN). PCR was done on ABI 7500 (Applied Biosystems) or Step-One Plus (Applied Biosystems) with TaqMan Universal PCR Master Mix (Applied Biosystems). Relative amounts of mRNA were calculated by the comparative ΔC(t) method. TaqMan Gene expression assays for qPCR, including *Bmp4* (Mm00432087_m1), *Foxn1* (Mm00433948_m1), *Bmpr1a* (Mm00477650_m1), *Bmpr1b* (Mm03023971_m1), *Bmpr2* (Mm00432134_m1), *Dll4* (Mm00444619_m1), *Kitl* (Mm00442972_m1) and *Cxcl12* (Mm00445553_m1) were all purchased from Life Technologies (Carlsbad, CA).

shRNA

To silence BMP4, $exEC^{(Thymus)}$ were incubated in 8μg/ml polybrene with a lentiviral construct containing *Bmp4* shRNA or scrambled sequences encoding for target specific 19–25nt shRNA with a 6bp loop (sc-39745-V purchased from Santa Cruz Biotechnology, Dallas, Tx). After 5 days, puromycin (2μg/ml) was added to select for transduced cells.

Microscopy

Light-sheet field microscopy was performed as previously described (69). Briefly, PFA-fixed organs were dehydrated with increasing concentrations of ethanol and cleared with benzyl benzoate to benzyl alcohol at a 2: ratio. The organs were captured by a custom-built laser scanned light sheet fluorescence microscope at 20× magnification (0.95 NA) and stitched using FIJI image analysis software. Volumes were calculated using Imaris Software (Bitplane, Zurich CH) by segmenting an autofluorescence channel and the VE-Cadherin signal. Subsequent filament analysis using the module MeasurementPro yielded the vessel characterization measures where segments were defined as the length of vessel separating

two branching points. Data were exported for analysis with Matlab (Mathworks, Natick (MA), USA).

Statistics

Statistical analysis between two groups was performed with the nonparametric, unpaired Mann-Whitney *U* test. Statistical comparison between 3 or more groups was performed with the nonparametric, unpaired Kruskall-Wallis test. In Fig. 4J & 4L, statistics were generated using a two-way ANOVA with Tukey's multiple comparison test. All statistics were calculated using Graphpad Prism and display graphs were generated in Graphpad Prism or R.

Supplementary Material

Refer to Web version on PubMed Central for supplementary material.

Acknowledgments

We gratefully acknowledge the bioinformatics assistance of Anastasia Kousa; the technical assistance of Frances Maher and Ysabel Ojoylan; the Research Animal Resource Center and the Flow Cytometry Core at MSKCC; the Emerging Global Diseases Flow Cytometry Facility at the University of Georgia; and the Flow Cytometry and Comparative Medicine Core Facilities at the Fred Hutchinson Cancer Research Center.

Funding: This study was supported by NIH grants R00-CA176376 (to J.A.D.), P01-AG052359/Project 2 (Janko Nikolich-Zugich/M.R.M.vdB., J.D.), R01-HL069929, R01-AI100288, R01-AI080455, and R01-AI101406 (to M.R.M.vdB.), P01-CA023766/Project 4 (Richard J. O'Reilly/M.R.M.vdB.), P30-CA008748 (MSKCC Core Grant), P30-CA15704 (FHCRC Core Grant), and by a subcontract from RFP-NIAID-DAIT-NIHAI2008023 (N.R.M.). Support was also received from The Lymphoma Foundation (M.R.M.vdB.), The Susan and Peter Solomon Divisional Genomics Program (M.R.M.vdB.), MSKCC Cycle for Survival (M.R.M.vdB.), the Cuyamaca Foundation (J.A.D.), and the Bezos Family Foundation (J.A.D.). This project has received funding from the European Union's Seventh Programme for research, technological development and demonstration under grant agreement No [602587]. J.A.D. was also supported by a Scholar Award from the American Society of Hematology, and the Mechtild Harf Award from the DKMS Foundation for Giving Life. T.W. was supported by a Boehringer Ingelheim Fonds MD fellowship and by the German National Academic Foundation. C.C.K. is a Prostate Cancer Foundation Young Investigator. K.O., C.B., Z.M., and A.B. were supported by a grant from the IZKF Wurzburg (B233).

Competing interests: J.D., T.W., and M.vdB. are inventors on a patent application (US2015/058095) submitted by Memorial Sloan Kettering Cancer Center that covers the use of ECs and/or BMP4 for thymic regeneration. S.R. is a founder of (and unpaid consultant to), and D.N. and M.G. are employees of, Angiocrine Biosciences; which holds patents on the platform technology surrounding E4ORF1 expression in ECs.

REFERENCES AND NOTES

1. Abramson J, Anderson G. Thymic Epithelial Cells. Annu Rev Immunol. 2017
2. Chaudhry MS, Velardi E, Dudakov JA, van den Brink MRM. Thymus: the next (re)generation. Immunological Reviews. 2016; 271:56–71. [PubMed: 27088907]
3. Jaffe HL. The Influence of the Suprarenal Gland on the Thymus: I. Regeneration of the Thymus Following Double Suprarenalectomy in the Rat. J Exp Med. 1924; 40:325–342. [PubMed: 19868921]
4. Miller JF. Immunological function of the thymus. Lancet. 1961; 2:748–749. [PubMed: 14474038]
5. Dudakov, JA., Perales, MA., van den Brink, MRM. Thomas' Hematopoietic Cell Transplantation. Forman, S.Negrin, RS.Antin, JH., Appelbaum, FA., editors. Vol. 1. John Wiley & Sons, Ltd; West Sussex, UK: 2016. p. 160-165.chap. 2B
6. Bosch M, Khan FM, Storek J. Immune reconstitution after hematopoietic cell transplantation. Curr Opin Hematol. 2012; 19:324–335. [PubMed: 22517587]

7. Chinn IK, Blackburn CC, Manley NR, Sempowski GD. Changes in primary lymphoid organs with aging. Semin Immunol. 2012; 24:309–320. [PubMed: 22559987]
8. Dudakov JA, et al. Interleukin-22 Drives Endogenous Thymic Regeneration in Mice. Science. 2012; 336:91–95. [PubMed: 22383805]
9. Bleul CC, Boehm T. BMP signaling is required for normal thymus development. Journal of Immunology. 2005; 175:5213–5221.
10. Chen D, Zhao M, Mundy GR. Bone morphogenetic proteins. Growth Factors. 2004; 22:233–241. [PubMed: 15621726]
11. Sun X, et al. Directed Differentiation of Human Embryonic Stem Cells into Thymic Epithelial Progenitor-like Cells Reconstitutes the Thymic Microenvironment In†Vivo. Cell Stem Cell. 2013; 13:230–236. [PubMed: 23910085]
12. Parent AV, et al. Generation of functional thymic epithelium from human embryonic stem cells that supports host T cell development. Cell Stem Cell. 2013; 13:219–229. [PubMed: 23684540]
13. Tsai PT, Lee RA, Wu H. BMP4 acts upstream of FGF in modulating thymic stroma and regulating thymopoiesis. Blood. 2003; 102:3947–3953. [PubMed: 12920023]
14. Nehls M, et al. Two genetically separable steps in the differentiation of thymic epithelium. Science. 1996; 272:886–889. [PubMed: 8629026]
15. Chen L, Xiao S, Manley NR. Foxn1 is required to maintain the postnatal thymic microenvironment in a dosage-sensitive manner. Blood. 2009; 113:567–574. [PubMed: 18978204]
16. Bredenkamp N, et al. An organized and functional thymus generated from FOXN1-reprogrammed fibroblasts. Nat Cell Biol. 2014; 16:902–908. [PubMed: 25150981]
17. Blackburn CC, et al. The nu gene acts cell-autonomously and is required for differentiation of thymic epithelial progenitors. Proceedings of the National Academy of Sciences of the United States of America. 1996; 93:5742–5746. [PubMed: 8650163]
18. Bredenkamp N, Nowell CS, Blackburn CC. Regeneration of the aged thymus by a single transcription factor. Development. 2014; 141:1627–1637. [PubMed: 24715454]
19. Zook EC, et al. Overexpression of Foxn1 attenuates age-associated thymic involution and prevents the expansion of peripheral CD4 memory T cells. Blood. 2011; 118:5723–5731. [PubMed: 21908422]
20. Calderon L, Boehm T. Synergistic, Context-Dependent, and Hierarchical Functions of Epithelial Components in Thymic Microenvironments. Cell. 2012; 149:159–172. [PubMed: 22464328]
21. Zuklys S, et al. Foxn1 regulates key target genes essential for T cell development in postnatal thymic epithelial cells. Nat Immunol. 2016; 17:1206–1215. [PubMed: 27548434]
22. Bajoghli B, et al. Evolution of genetic networks underlying the emergence of thymopoiesis in vertebrates. Cell. 2009; 138:186–197. [PubMed: 19559469]
23. Wang Y, et al. Ephrin-B2 controls VEGF-induced angiogenesis and lymphangiogenesis. Nature. 2010; 465:483–486. [PubMed: 20445537]
24. Zhang SL, et al. Chemokine treatment rescues profound T-lineage progenitor homing defect after bone marrow transplant conditioning in mice. Blood. 2014; 124:296–304. [PubMed: 24876562]
25. Cuddihy AR, et al. Rapid thymic reconstitution following bone marrow transplantation in neonatal mice is VEGF-dependent. Biol Blood Marrow Transplant. 2012; 18:683–689. [PubMed: 22281302]
26. Ding BS, et al. Endothelial-derived angiocrine signals induce and sustain regenerative lung alveolarization. Cell. 2011; 147:539–553. [PubMed: 22036563]
27. Ding BS, et al. Inductive angiocrine signals from sinusoidal endothelium are required for liver regeneration. Nature. 2010; 468:310–315. [PubMed: 21068842]
28. Rafii S, Butler JM, Ding BS. Angiocrine functions of organ-specific endothelial cells. Nature. 2016; 529:316–325. [PubMed: 26791722]
29. Seandel M, et al. Generation of a functional and durable vascular niche by the adenoviral E4ORF1 gene. Proceedings of the National Academy of Sciences of the United States of America. 2008; 105:19288–19293. [PubMed: 19036927]

30. Zhang F, et al. Adenovirus E4 gene promotes selective endothelial cell survival and angiogenesis via activation of the vascular endothelial-cadherin/Akt signaling pathway. The Journal of biological chemistry. 2004; 279:11760–11766. [PubMed: 14660586]
31. Nolan DJ, et al. Molecular signatures of tissue-specific microvascular endothelial cell heterogeneity in organ maintenance and regeneration. Developmental cell. 2013; 26:204–219. [PubMed: 23871589]
32. Buono M, et al. A dynamic niche provides Kit ligand in a stage-specific manner to the earliest thymocyte progenitors. Nat Cell Biol. 2016; 18:157–167. [PubMed: 26780297]
33. Hozumi K, et al. Delta-like 4 is indispensable in thymic environment specific for T cell development. J Exp Med. 2008; 205:2507–2513. [PubMed: 18824583]
34. Koch U, et al. Delta-like 4 is the essential, nonredundant ligand for Notch1 during thymic T cell lineage commitment. J Exp Med. 2008; 205:2515–2523. [PubMed: 18824585]
35. Patel SR, Gordon J, Mahbub F, Blackburn CC, Manley NR. Bmp4 and Noggin expression during early thymus and parathyroid organogenesis. Gene Expression Patterns. 2006; 6:794–799. [PubMed: 16517216]
36. Gordon J, Patel SR, Mishina Y, Manley NR. Evidence for an early role for BMP4 signaling in thymus and parathyroid morphogenesis. Dev Biol. 2010; 339:141–154. [PubMed: 20043899]
37. Soh CL, et al. FOXN1GFP/w Reporter hESCs Enable Identification of Integrin- β4, HLA-DR, and EpCAM as Markers of Human PSC-Derived FOXN1+ Thymic Epithelial Progenitors. Stem Cell Reports. 2014; 2:925–937. [PubMed: 24936476]
38. Cai J, Lee J, Kopan R, Ma L. Genetic interplays between Msx2 and Foxn1 are required for Notch1 expression and hair shaft differentiation. Dev Biol. 2009; 326:420–430. [PubMed: 19103190]
39. Vaidya HJ, Briones Leon A, Blackburn CC. FOXN1 in thymus organogenesis and development. Eur J Immunol. 2016; 46:1826–1837. [PubMed: 27378598]
40. Swann, Jeremy B., et al. Conversion of the Thymus into a Bipotent Lymphoid Organ by Replacement of Foxn1 with Its Paralog, Foxn4. Cell Reports. 2014; 8:1184–1197. [PubMed: 25131198]
41. Corbeaux T, et al. Thymopoiesis in mice depends on a Foxn1-positive thymic epithelial cell lineage. Proceedings of the National Academy of Sciences. 2010; 107:16613–16618.
42. Nowell CS, et al. Foxn1 regulates lineage progression in cortical and medullary thymic epithelial cells but is dispensable for medullary sublineage divergence. PLoS Genet. 2011; 7:e1002348. [PubMed: 22072979]
43. Cheng L, et al. Postnatal tissue-specific disruption of transcription factor FoxN1 triggers acute thymic atrophy. The Journal of biological chemistry. 2010; 285:5836–5847. [PubMed: 19955175]
44. Rode I, et al. Foxn1 Protein Expression in the Developing, Aging, and Regenerating Thymus. J Immunol. 2015
45. Song Y, et al. FOXN1 recombinant protein enhances T-cell regeneration after hematopoietic stem cell transplantation in mice. European Journal of Immunology. 2016 n/a-n/a.
46. Velardi E, et al. Sex steroid blockade enhances thymopoiesis by modulating Notch signaling. The Journal of Experimental Medicine. 2014; 211:2341–2349. [PubMed: 25332287]
47. Ding BS, et al. Divergent angiocrine signals from vascular niche balance liver regeneration and fibrosis. Nature. 2014; 505:97–102. [PubMed: 24256728]
48. Butler JM, et al. Endothelial Cells Are Essential for the Self-Renewal and Repopulation of Notch-Dependent Hematopoietic Stem Cells. Cell Stem Cell. 2010; 6:251–264. [PubMed: 20207228]
49. Hooper AT, et al. Engraftment and Reconstitution of Hematopoiesis Is Dependent on VEGFR2-Mediated Regeneration of Sinusoidal Endothelial Cells. Cell Stem Cell. 2009; 4:263–274. [PubMed: 19265665]
50. Kobayashi H, et al. Angiocrine factors from Akt-activated endothelial cells balance self-renewal and differentiation of haematopoietic stem cells. Nat Cell Biol. 2010; 12:1046–1056. [PubMed: 20972423]
51. Butler JM, et al. Development of a vascular niche platform for expansion of repopulating human cord blood stem and progenitor cells. Blood. 2012; 120:1344–1347. [PubMed: 22709690]

52. Bryson JL, et al. Cell-autonomous defects in thymic epithelial cells disrupt endothelial-perivascular cell interactions in the mouse thymus. PLoS One. 2013; 8:e65196. [PubMed: 23750244]
53. Muller SM, et al. Gene targeting of VEGF-A in thymus epithelium disrupts thymus blood vessel architecture. Proceedings of the National Academy of Sciences of the United States of America. 2005; 102:10587–10592. [PubMed: 16027358]
54. Baik S, Jenkinson EJ, Lane PJ, Anderson G, Jenkinson WE. Generation of both cortical and Aire(+) medullary thymic epithelial compartments from CD205(+) progenitors. Eur J Immunol. 2013; 43:589–594. [PubMed: 23299414]
55. Ulyanchenko S, et al. Identification of a Bipotent Epithelial Progenitor Population in the Adult Thymus. Cell Reports. 2016; 14:2819–2832. [PubMed: 26997270]
56. Wong K, et al. Multilineage Potential and Self-Renewal Define an Epithelial Progenitor Cell Population in the Adult Thymus. Cell Reports. 2014; 8:1198–1209. [PubMed: 25131206]
57. Rode I, Boehm T. Regenerative capacity of adult cortical thymic epithelial cells. Proceedings of the National Academy of Sciences. 2012; 109:3463–3468.
58. Mayer CE, et al. Dynamic spatio-temporal contribution of single beta5t+ cortical epithelial precursors to the thymus medulla. Eur J Immunol. 2016; 46:846–856. [PubMed: 26694097]
59. Barsanti M, et al. A novel Foxn1eGFP/+ mouse model identifies Bmp4-induced maintenance of Foxn1 expression and thymic epithelial progenitor populations. Eur J Immunol. 2016
60. Ohigashi I, et al. Adult Thymic Medullary Epithelium Is Maintained and Regenerated by Lineage-Restricted Cells Rather Than Bipotent Progenitors. Cell Rep. 2015; 13:1432–1443. [PubMed: 26549457]
61. Larsson J, Karlsson S. The role of Smad signaling in hematopoiesis. Oncogene. 2005; 24:5676–5692. [PubMed: 16123801]
62. Lis R, et al. Conversion of adult endothelium to immunocompetent haematopoietic stem cells. Nature. 2017; 545:439–445. [PubMed: 28514438]
63. Zlotoff DA, et al. Delivery of progenitors to the thymus limits T-lineage reconstitution after bone marrow transplantation. Blood. 2011; 118:1962–1970. [PubMed: 21659540]
64. Hager-Theodorides AL, et al. Bone morphogenetic protein 2/4 signaling regulates early thymocyte differentiation. J Immunol. 2002; 169:5496–5504. [PubMed: 12421925]
65. Hager-Theodorides AL, et al. Direct BMP2/4 signaling through BMP receptor IA regulates fetal thymocyte progenitor homeostasis and differentiation to CD4+CD8+ double-positive cell. Cell Cycle. 2014; 13:324–333. [PubMed: 24240189]
66. Varas A, et al. Interplay between BMP4 and IL-7 in human intrathymic precursor cells. Cell Cycle. 2009; 8:4119–4126. [PubMed: 19923894]
67. Cejalvo T, et al. Bone morphogenetic protein-2/4 signalling pathway components are expressed in the human thymus and inhibit early T-cell development. Immunology. 2007; 121:94–104. [PubMed: 17425602]
68. Norrie JL, et al. Dynamics of BMP signaling in limb bud mesenchyme and polydactyly. Dev Biol. 2014; 393:270–281. [PubMed: 25034710]
69. Brede C, et al. Mapping immune processes in intact tissues at cellular resolution. J Clin Invest. 2012; 122:4439–4446. [PubMed: 23143304]

ONE SENTENCE SUMMARY

BMP4 produced by endothelial cells promotes thymic regeneration after acute damage by activating FOXN1 and its downstream targets

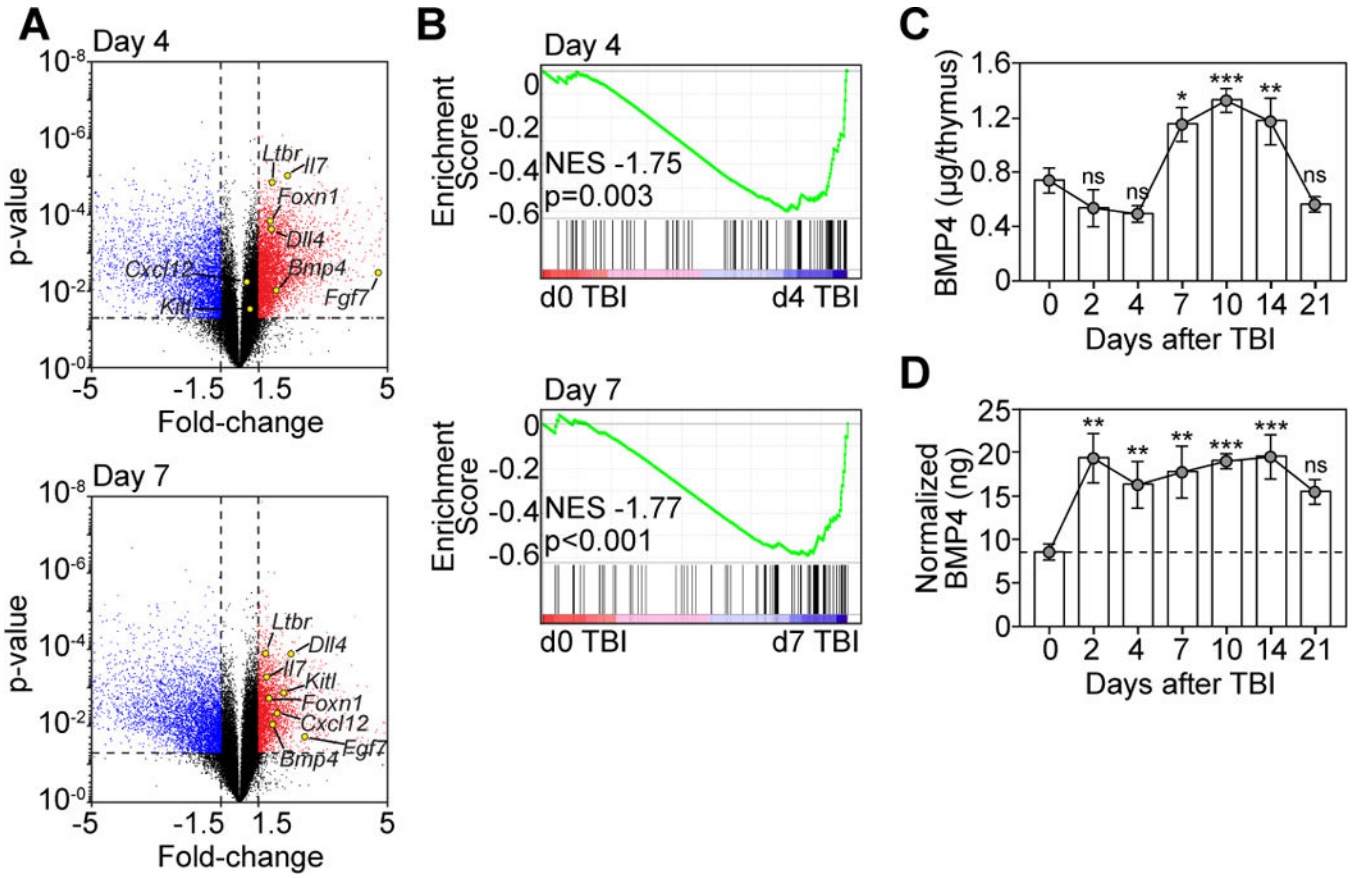

Figure 1. BMP signaling pathways are upregulated in the thymus after thymic damage

(A–B) Thymuses were pooled 6-week-old C57BL/6 mice and microarray analysis was performed on CD45$^-$ cells enriched from either untreated mice (d0) or 4, and 7 days after TBI (550 cGy, n=3/timepoint with each n pooled from 3–5 mice). (**A**) Volcano plot outlining genes that changed >1.5 fold, p<0.05 with some key thymus-related genes highlighted. (**B**) GSEA analysis was performed on the transcriptome derived from CD45$^-$ cells after TBI (Fig. 1A) with BMP target genes (GO: 0030510). (**C–D**) Thymuses were harvested at days 0, 2, 4, 7, 10, 14, and 21 after TBI (n=5–14/timepoint) and BMP4 levels were measured by ELISA. (**C**) Absolute amount of BMP4 in the thymus. (**D**) Amount of BMP4 normalized to the weight of the thymus (ng BMP4/µg thymus). Data combined from 2–3 independent experiments. *, p<0.05; **, p<0.01, ***, p<0.001.

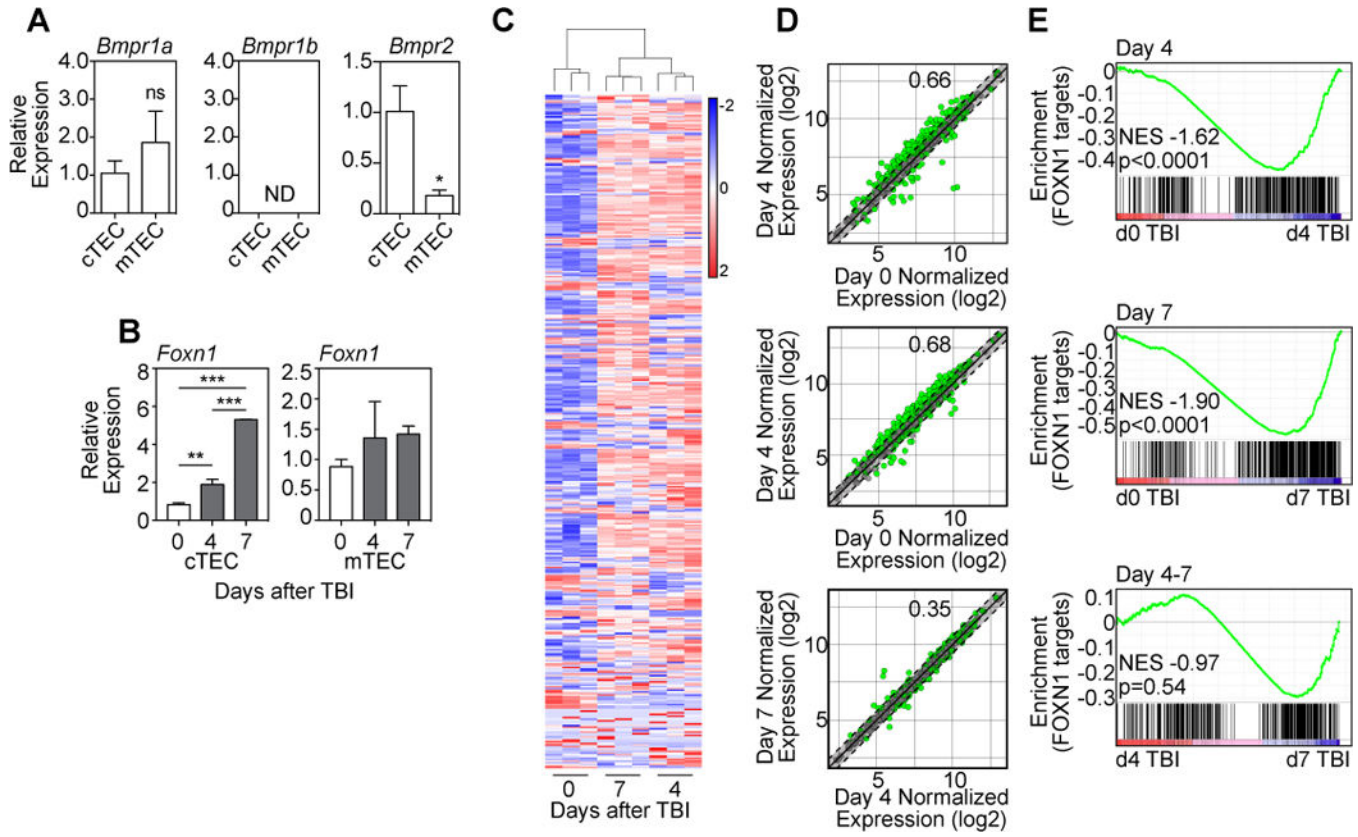

Figure 2. BMP4 targets thymic epithelial cells and induces expression of *Foxn1* and its downstream targets after damage

(**A**) TEC subsets were FACS purified from untreated 6 week-old C57BL/6 mice and expression of the BMPR subunits *Bmpr1a, Bmpr1b*, and *Bmpr2* were measured by qPCR (n=3/subset). (**B**) cTECs or mTECs were FACS purified from the thymus at days 0, 4 and 7 after TBI and expression of *Foxn1* was assessed by qPCR (n=4–6/timepoint from 2–3 independent experiments). (**C–E**) Thymuses were pooled from 6 week-old C57BL/6 mice and microarray analysis was performed on $CD45^-$ cells enriched from either untreated mice (d0) or 4, and 7 days after TBI (550 cGy, n=3/timepoint with each n pooled from 3–5 mice). (**C**) Heat map of high confidence FOXN1 target genes in cTECs (21) showing clustering between samples and between days 0, 4 and 7. (**D**) Dot plots showing normalized expression values comparing days 0, 4 and 7 after TBI. Green dots represent individual genes significantly different ($p<0.05$), and dotted lines (and shaded section) represent genes with a fold change <1.5 (+/−). The proportion of significantly changed genes is denoted within each plot. (**E**) GSEA analysis was performed comparing gene changes with a FOXN1 target gene signature comprising the list of high confidence FOXN1 gene targets (Table S1). Bar graphs represent mean ± SEM. *, $p<0.05$; **, $p<0.01$, ***, $p<0.001$.

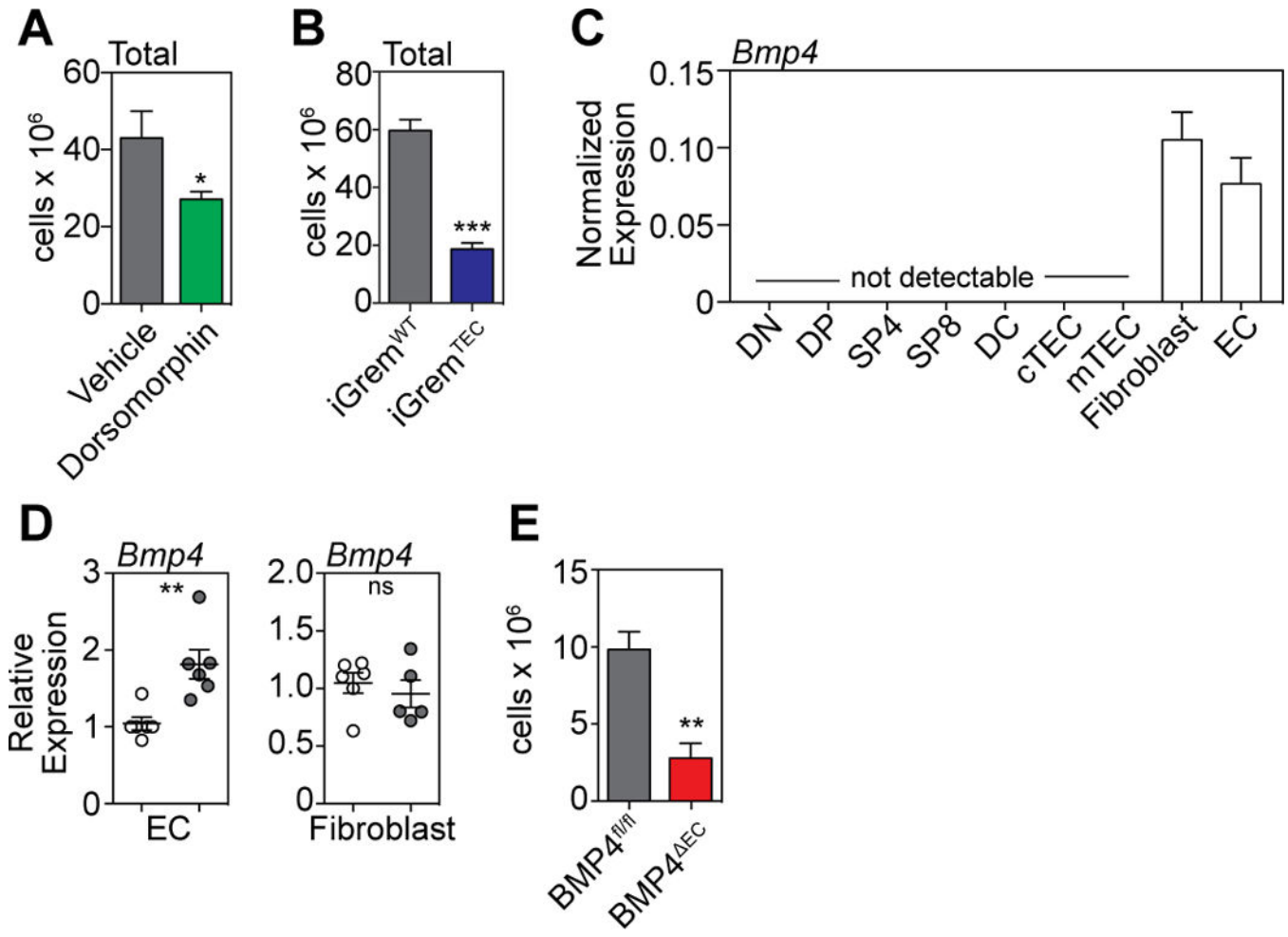

Figure 3. BMP4 production by ECs represents a non-redundant pathway of regeneration after thymic damage

(**A**) Six week old C57BL/6 mice were administered with the BMP type I receptor inhibitor Dorsomorphin dihydrochloride (12.5mg/kg) i.p. at day −1 before TBI and twice daily after TBI. Thymus was harvested and total cellularity assessed at day 7 after TBI (n=10 mice/treatment). (**B**) Tamoxifen was administered to iGremlin::K5-CreER^{+}(iGrem^{TEC}) and iGremlin::K5-CreER^{-} (iGrem^{WT}) mice on days −1, 0 and +1 surrounding TBI (550cGy). Thymus was harvested and total cellularity assessed on day 9. (**C**) Cell subsets (n=3/population) comprising approximately 99.5% of the known cellular subsets in the thymus were FACS purified and assessed for their expression of *Bmp4* at steady-state by qPCR: double negative (DN, CD4-CD8−), double positive (DP, CD4+CD8+), single positive (SP)-4 (CD4+CD8-CD3+), SP8 (CD4^{-}CD8^{+}CD3^{+}), dendritic cells (DC, CD11c^{+}MHCII^{+}), cTEC (CD45^{-}EpCAM^{+}MHCII^{+}Ly51^{+}UEA1^{lo}), mTEC (CD45^{-}EpCAM^{+}MHCII^{+}Ly51^{lo}UEA1^{+}), Fibroblasts (CD45^{-}EpCAM^{-}PDGFRa^{+}), ECs (CD45^{-}EpCAM^{-}VE-Cad^{+}). (**D**) ECs and Fibroblasts were FACS sorted at days 0 and 4 after TBI and expression of *Bmp4* was assessed by qPCR (n=6/population/timepoint). (**E**) Tamoxifen was administered to BMP4$^{fl/fl}$::Cdh5-CreERT2^{+} (BMP4$^{\Delta EC}$, n=18) and BMP4$^{fl/fl}$::Cdh5-CreERT2^{-} (BMP4$^{fl/fl}$, n=17) mice on days −2, −1, 0, 1 and 2 surrounding TBI (550cGy). Thymus was harvested

and total cellularity measured on day 7. Bar graphs represent mean ± SEM of at least 2 independent experiments. *, $p<0.05$; **, $p<0.01$, ***, $p<0.001$.

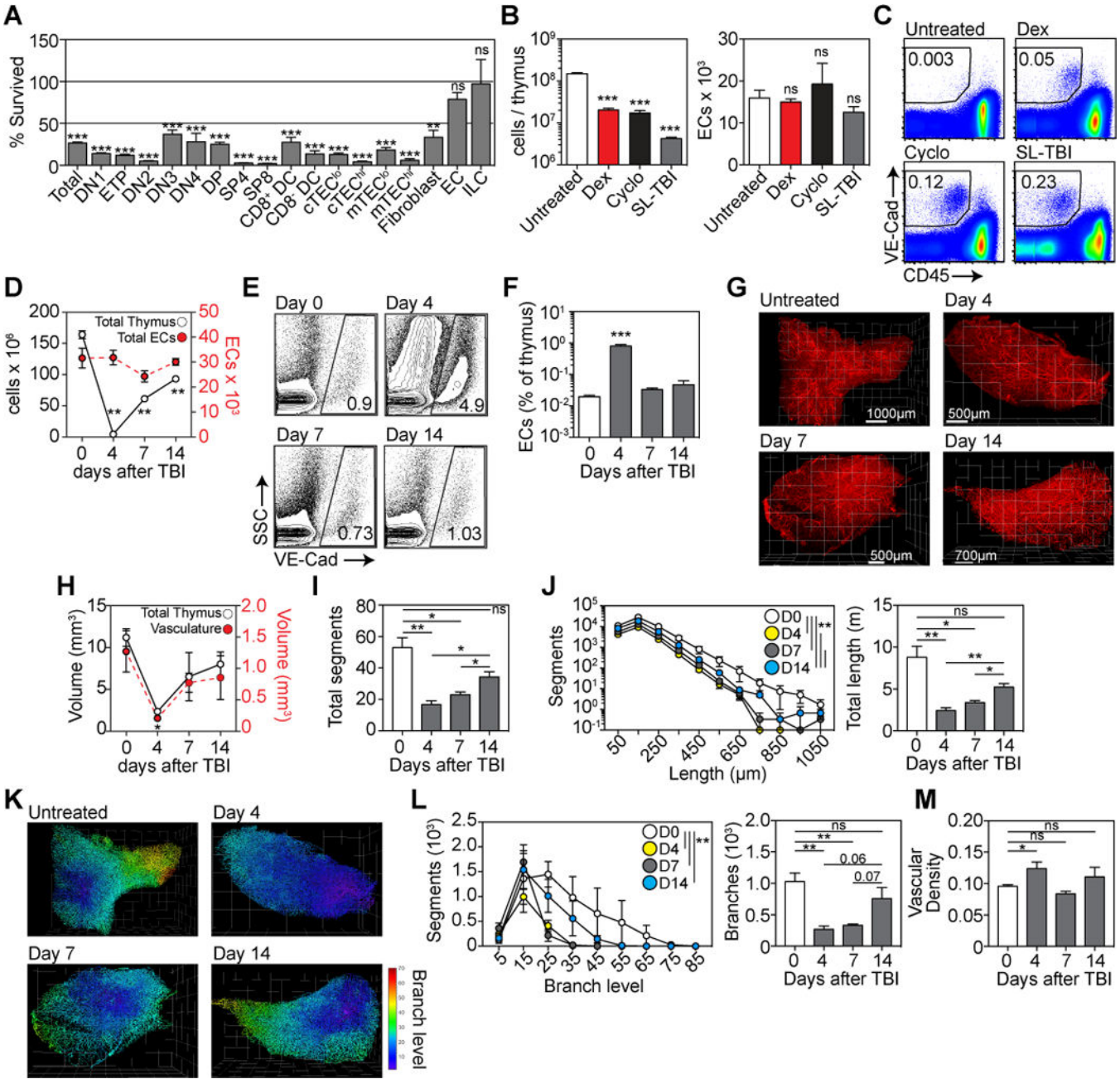

Figure 4. Endothelial cells form a damage-resistant regenerative niche in the thymus

(**A**) Cell subsets in the thymus were assessed at day 7 after TBI and the depletion calculated compared to an untreated age-matched control cohort (n=10–25/subset). Subsets analyzed include DN1 ($CD44^+CD25^-$), ETP (($CD44^+CD25^-ckit^+$), DN2 (($CD44^+CD25^-$), DN3 ($CD44^+CD25^-$), DN4 ($CD44^+CD25^-$), DP, SP4, SP8, $CD8^+$ or $CD8^-$ DCs, $MHCII^{hi}$ or $MHCII^{lo}$ $cTEC^{hi/lo}$ ($CD45^-EpCAM^+MHCII^+Ly51^+UEA1^{lo}$), $MHCII^{hi}$ or $MHCII^{lo}$ $mTEC^{hi/lo}$ ($CD45^-EpCAM^+MHCII^+Ly51^{lo}UEA1^+$), fibroblast, ECs, and innate lymphoid cells ($CD45^+CD3^-CD8$-$IL7R\alpha^+CD4^+ROR\gamma t^+CCR6^+$). (**B–C**) 6 week-old female C57BL/6 mice were treated with PBS (n=10), Dexamethasone (Dex, 50mg/kg ip on day 0, n=10),

cyclophosphamide (Cyclo, 100mg/kg/day ip on days −1 and 0, n=10) or TBI (550 cGy on day 0, n=10). On day 4, mice were perfused with 25μg anti-VE-cadherin antibody (BV13) conjugated to Alexa 647 sacrificed and total thymic cellularity and endothelial cell number assessed. (**B**) Total thymic cellularity and absolute number of ECs. (**C**) Concatenated flow cytometry plots detailing the proportion of VE-Cadherin+CD45− cells in the thymus. (**D–E**), C57BL/6 mice were given TBI (n=10–15/group) and assessed on days 4, 7 and 14. On the day of harvest mice were perfused with 25μg anti-VE-cadherin antibody (BV13) conjugated to Alexa 647. (**D**) Total cellularity (open circles) and absolute number of endothelial cells (closed circles) in the thymus calculated using flow cytometry. (**E**) Proportion of VE-cadherin^{+} ECs as a function of CD45-stromal cells. Flow cytometry plots represent concatenated data from one experiment. (**F**) Proportion of ECs as a function of total thymic cellularity (n=14–20 from 4 independent experiments). (**G**–**M**) 3D reconstruction of thymus vasculature at days 0, 4, 7 and 14 after TBI using light sheet field microscopy (n=3/timepoint). (**G**) Visualization of VE-Cadherin staining in the thymus. (**H**) Calculation of the volume of whole thymus and vasculature. (**I**) Total number of vessel segments in the thymus vasculature after damage where segments were defined as the length of vessel between two branching points. (**J**) Vessel segments were binned according to their length. Total vasculature length was calculated. (**K**) Vascular segments were color-coded based on branch level. (**L**) Number of segments/branch level and the total number of vessel branches. (**M**) Vascular density was calculated as a ratio of vascular network volume as a function of total thymus volume (from Fig. 4H). Bar graphs represent mean ± SEM. *, $p<0.05$; **, $p<0.01$, ***, $p<0.001$.

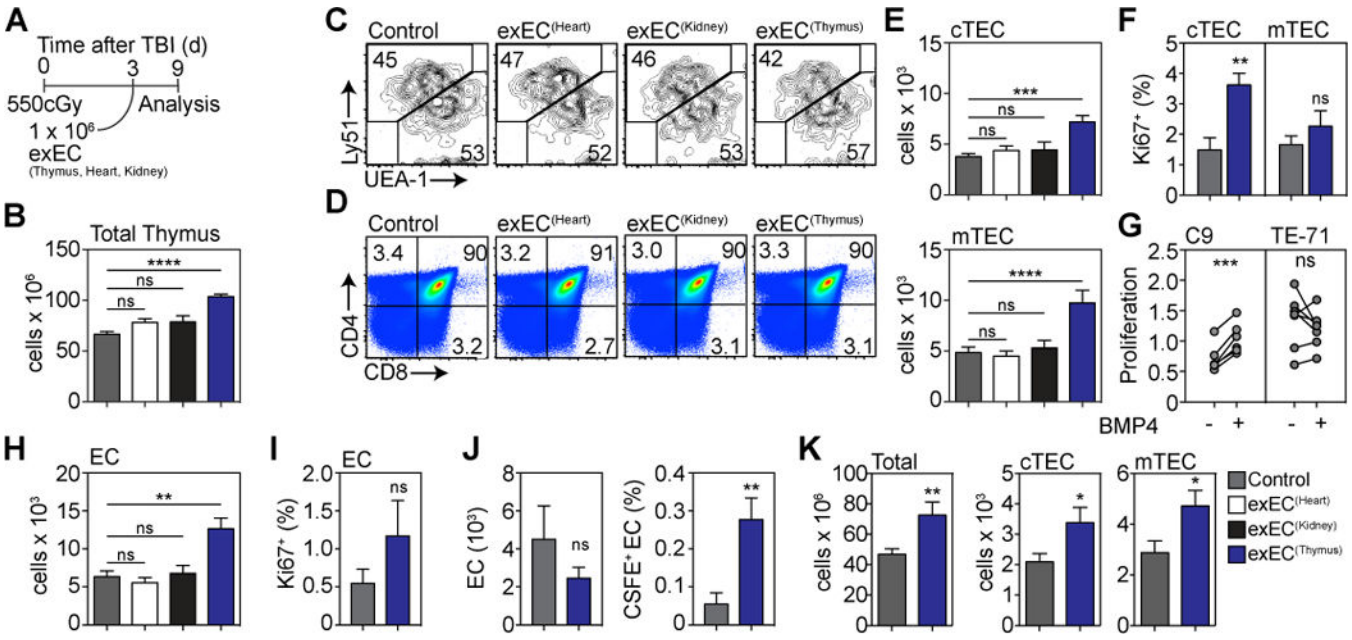

Figure 5. Thymic ECs can be cultivated *ex vivo* and mediate enhanced thymic regeneration upon exogenous administration after damage

ECs were FACS sorted from the thymus (n=25), heart (n=10) or kidney (n=10) based on expression of VE-cadherin and transduced with the viral gene E4ORF1. These cells are referred to as exEC. In order to model immune injury we exposed 6–8 week-old C57BL/6 mice to TBI and 1 × 10^6 exEC were administered iv at day 3 after TBI (n=25 in control group). (**A**) Experiment schematic. (**B**) Total thymic cellularity at day 9 after TBI. (**C–D**) Concatenated flow cytometric plots detailing the proportion of (**C**) TECs and (**D**) thymocyte subsets. (**E**) Absolute number of cortical and medullary thymic epithelial cells (cTEC and mTEC respectively). (**F**) TEC proliferation was measured on day 3 by Ki-67 staining. (**G**) C9 or TE-71 cells were stimulated with BMP4 (100ng/ml) for 24 hours after which proliferation was assessed (n=6–7 independent experiments). (**H**) Absolute number of ECs. (**I**) EC proliferation on day 3 after exEC administration. (**J**) exECs were generated and labeled with CFSE and 10 × 10^6 cells were transferred on day 3 after TBI. 4 hours after transfer CFSE expression was assessed by VE-Cad$^+$ cells in the thymus. Displayed are total EC number and proportion of CFSE$^+$ ECs (n=13–15 from three independent experiments). (**K**) Total thymic cellularity and absolute number of cTEC and mTEC 28 days after TBI and administration of 1 × 10^6 thymus-derived exEC on day 3 (n=10/group). Graphs represent mean ± SEM of at least 2 independent experiments. *, p<0.05; **, p<0.01, ***, p<0.001.

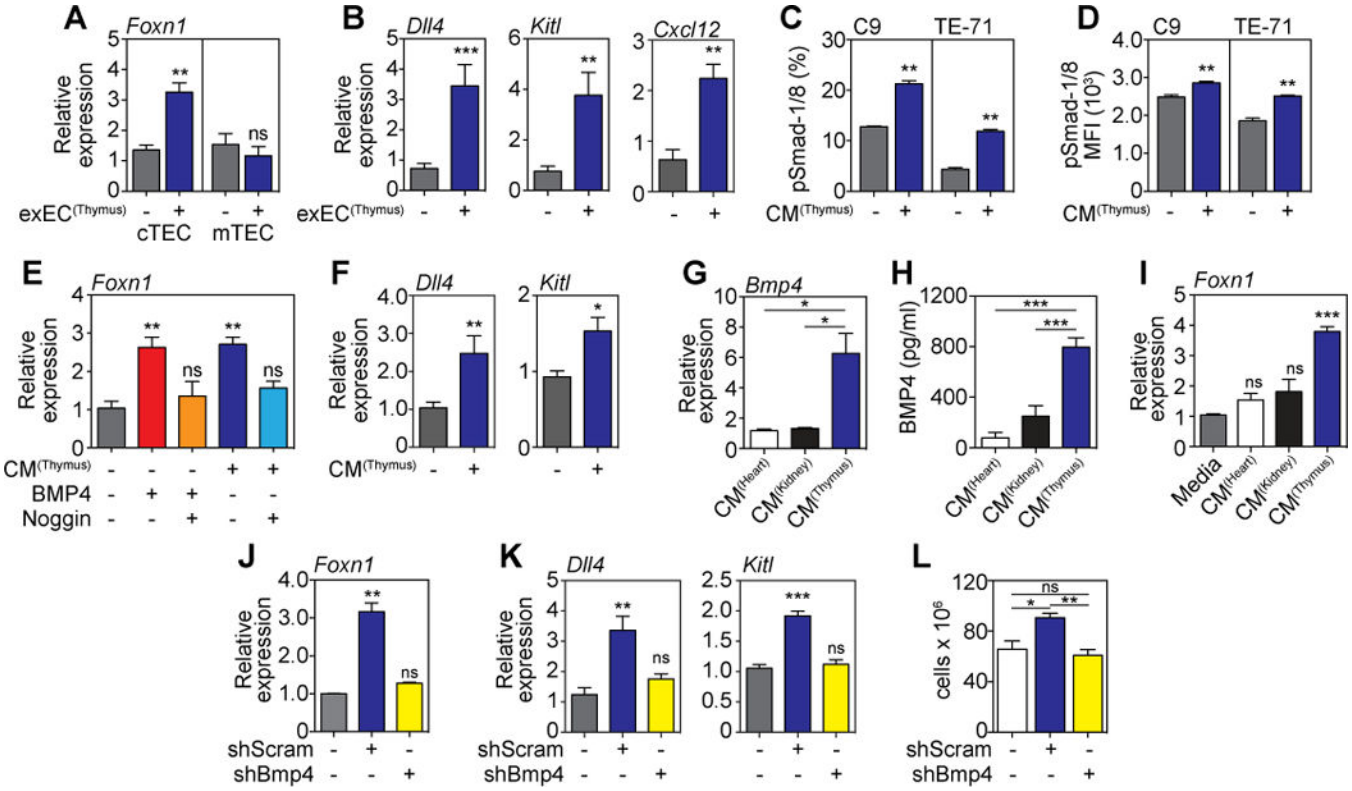

Figure 6. exEC-produced BMP4 mediates thymic regeneration via activation of Foxn1 in TECs

(**A–B**) 6–8 week-old C57BL/6 mice were given TBI and 1 × 10^6 exEC were administered iv at day 3 after TBI. Thymus was harvested 4 days later and cortical and medullary TECs were FACS purified and expression of *Foxn1* (**A**) and its downstream target genes *Dll4, Kitl*, and *Cxcl12* in cTECs (**B**) was measured by qPCR (n=8–9/group). (**C–D**) Conditioned media (CM) from *in vitro* cultures of exEC derived from thymus was incubated with C9 or TE-71 cells for 20 minutes after which phosphorylation of Smad1/8 was measured by flow cytometry (n=3/group). (**E–F**) CM from *in vitro* cultures of exEC derived from thymus was incubated with the cTEC cell line C9 for 24 hours (n=7–10). Recombinant BMP4 (30ng/ml) or and/or Noggin (100ng/ml) were added to marked wells as controls. (**E**) *Foxn1* measured by qPCR. (**F**) Expression of *Dll4 and Kitl* measured by qPCR. (**G**) *Bmp4* expression in heart, kidney and thymus exEC. (**H**) BMP4 protein was measured by ELISA in exEC CM derived from thymus, heart or kidney (n=4/group). (**I**) CM from exEC generated from heart, kidney or thymus was incubated with C9 cells for 24 hours after which expression of *Foxn1* was measured by qPCR. (**J–L**) exEC were generated from thymus-derived ECs and transduced to express either a *Bmp4* shRNA (shBMP4) or scrambled (shScram) control. (**J–K**) CM derived from thymus shBMP4 or shScram exEC cultures was incubated with C9 cells for 24 hours when *Foxn1* (**J**) and or the Foxn1 downstream genes *Dll4* and *Kitl* (**K**) expression was assessed by qPCR. (**L**) Transduced exEC were transplanted into mice previously given TBI on day 3. Total thymus cellularity at day 9 after shBmp4 or shScram was administered 3 days after TBI (n=10/group). Bar graphs represent mean ± SEM of at least 2 independent experiments. *, p<0.05; **, p<0.01, ***, p<0.001.